Nonlinear Dyn (2007) 49:217–232
DOI 10.1007/s11071-006-9123-z

ORIGINAL ARTICLE

The bouncing motion appearing in a robotic system with unilateral constraint

Caishan Liu · Zhen Zhao · Bin Chen

Received: 15 December 2005 / Accepted: 9 August 2006 / Published online: 27 September 2006

Abstract The hopping or bouncing motion can be observed when robotic manipulators are sliding on a rough surface. Making clear the reason of generating such phenomenon is important for the control and dynamical analysis for mechanical systems. In particular, such phenomenon may be related to the problem of Painlevé paradox. By using LCP theory, a general criterion for identifying the bouncing motion appearing in a planar multibody system subject to single unilateral constraint is established, and found its application to a two-link robotic manipulator that comes in contact with a rough constantly moving belt. The admissible set in state space that can assure the manipulator keeping contact with the rough surface is investigated, and found which is influenced by the value of the friction coefficient and the configuration of the system. Painlevé paradox can cause either multiple solutions or non-existence of solutions in calculating contact force. Developing some methods to fill in the flaw is also important for perfecting the theory of rigid-body dynamics. The properties of the tangential impact relating to the inconsistent case of Painlevé paradox have been discovered in this paper, and a jump rule for determining the post-states after the tangential impact finishes is developed. Finally, the comprehensively numerical simulation for the two-link robotic manipulator is carried out, and its dynamical behaviors such as stick-slip, the bouncing motion due to the tangential impact at contact point or the external forces, are exhibited.

Keywords Dynamical simulation · Friction · Painlevé paradox · Stick-slip · Tangential impact

C. Liu (✉) · Z. Zhao · B. Chen
Department of Mechanics and Engineering Science,
Peking University, Beijing 100871, China
e-mail: lcs@mech.pku.edu.cn

1 Introduction

Unilateral constraints combined with friction can result in many complex dynamical phenomena. A typical example relating to them is the control of keeping a robotic manipulator sliding on a rough surface which can be hampered by the instability bouncing motion. This paper will illustrate with an example of two-link manipulator system that such phenomena might be related to the classical problem of rigid-body dynamics, Painlvé's paradox [1].

In the classical Painlevé example where a planar rod slides on a rough plane, the paradoxical situations in using rigid-body model may appear in the dynamical equations when the value of friction coefficient is larger enough [1–3]. Historically, many authors had studied such problem and obtained a series of valuable conclusions [1–27]. However, there are still some ambiguous opinions and unsolved problems on the Painlevé paradox: (1) Since the value of friction coefficient is needed to be larger than 4/3 for the occurrence of paradoxical situation in the classical Painlevé example [11–15], the studies on the Painlevé paradox are often considered to

be nothing with the practical problems; (2) The failure of the solution in using rigid-body model can be attributed to the combination of the assumption of rigidity and the Coulomb friction law, so the discussion about whether the deformation ignored in the contact area or the limitation of Coulomb friction law itself is the main cause of resulting in paradoxical situation still exists [16, 17, 22]. (3) Painlevé paradox can cause either multiple solutions which is termed as indeterminacy, or non-existence of solutions which is called as inconsistency [13]. There are still some dispute about how to determine a reasonable solution by using rigid-body dynamical theory when paradox appears, particularly, in the case of inconsistency that is often thought to be related to a shock at the contact point [9, 12, 13, 18].

Leine et al. [14] fully studied the system of Frictional Impact Oscillator which exhibits the Painlevé paradox with physically realistic values of the friction coefficient. Paradoxical situations are also found in the brake system and the motion of a rotating shaft [25, 26]. Our study in this paper will show that the paradoxical situation may appear even in a very small value of friction coefficient. Therefore, the Painlevé paradox may be not only the theoretical problem in the framework of rigid-body dynamics, but can have significance on the explanation of many physical phenomena existing in mechanical systems.

Concerning the reason of resulting in paradoxical situation in using rigid-body model, Lötstedt [5, 6] discussed a simulation method by modifying the friction law. Grigoryan [22] restricted the maximum of the value of the friction force attained at large values of the normal force. However, these methods cannot virtually solve the problem of the Painlevé paradox since there is no enough evidence to explain the Coulomb law is inapplicable in the paradoxical situation. Ivanov [17] pointed out the "corrected" friction law shown in [22] even leads to additional singularities. Therefore, the deformation ignored on the contact area by using rigid-body model should be the main root of resulting in paradox.

To develop some methods of ruling out the paradoxical situation in using rigid-body model would require some senses of the physical phenomena corresponding to it. This can be only implemented by using the deformable elements methods [28, 29]. Among the simulations in [10, 16, 19, 21] of adopting the deformable elements methods, the similar global properties for the paradoxical cases in rigid-body model have been found: in the indeterminate case of the solutions, no normal force exists, and contact is immediately broken; while in the inconsistent case, the contact forces have the characteristic of impulse, and the contact will finally separate. Therefore, we can select the zero contact force as the reasonable solution for the case of indeterminacy, while consider the case of inconsistency relating to a shock at contact point [13, 23, 24]. However, the difficulty of how to determine the post-states after the shock finishes is still unsolved.

Many authors have realized the fact that the inconsistent case in Painlevé paradox is related to a shock at the contact point. Lecornu was the first one to propose velocity jumps to escape from the inconsistent modes in rigid-body model [13], often now addressed as impacts without collisions or tangential impacts [8, 18], but he did not provide an effective method of determining the post-speed after jumps. Wang and Mason [9] present a detailed discussion on single contact point collisions involving friction, and explain how to resolve the inconsistency by applying impulsive contact forces to the configuration. However, his method is limited to a planar rod. Some authors [10, 23, 24] systematically associate sticking as the solution to inconsistency. In other words, the contact impulse must be something that makes contact bodies not separate after the tangential impact finishes. This opinion is called into question by some other authors that they thought there is no reason for such sticking to occur. Brach [18] considered the value of the tangential post-impact velocity should essentially depend on a critical value of the impulse ratio. Ivanov [17] took either the velocity sticking or reversal to be alternative solutions for the tangential impact. Obviously, it is still ambiguous about how to determine the post-state when tangential impact occurs.

So there are still two important problems relating to the study of Painlevé paradox. The first one is how to establish a criterion for identifying the occurrence of paradox. Fortunately, such criterion can be established by using the linear complementarity theory [8], which is introduced by Glocker and Pheiffer [11] into the multibody dynamics. Once such criterion is developed, the causes of the bouncing motion appearing in a robotic system can be clear, and be important for the control of the robotic system [27]. In this paper, we will make attempt to establish such criterion for a planar multibody system with single unilateral constraint. Its application will be found in an example of two-link robotic manipulator that comes in contact with a

rough constantly moving belt. The connection between the bouncing motion existing in such system and the Painlevé paradox will also be investigated.

The other important problem on the study of Painlevé paradox is how to find a reasonable solution for the tangential impact. Although some authors make attempt to solve such problem by directly adopting the Newton's restitution coefficient to determine the post-states [12, 18], it seems unreasonable since the relative speed in normal direction at contact point equals zero before the tangential impact occurs. Considering the fact that tangential impact is related to a shock at contact point, in this paper we will use the Keller's method for dealing with the collision between two rough bodies to establish a set of differential impulsive equations [20, 30–33]. Such differential equations expressed in velocity-impulse space can help us to analyze the global properties of tangential impact, and to develop a velocity jump rule for the simulation when the paradoxical situation appears in using rigid-body model.

We present our study as follows. First, we will establish a general condition for identifying the occurrence of Painlevé paradox in a planar multibody system with single unilateral constraint. Such condition can help us to understand the causes of bouncing motion appearing in the robotic system. At the meantime, a definition of the admissible state set that the multibody system can sustain contact is presented. Second, for a two-link robotic manipulator touching on a rough moving belt, we will investigate the structure of the admissible set and its changes due to the shift of the value of friction coefficient. Third, we will study the properties of the tangential impact, and develop an effective method to rule out the paradoxical situation in using rigid-body model. Finally, numerical simulation are carried out for the robotic system, and abundant dynamical behaviors such as bouncing motion due to either the tangential impact or the external forces and the stick-slip phenomenon will be exhibited. Some conclusions are presented at the end of this paper.

2 The condition for the occurrence of bouncing motion

Suppose that the planar multi-rigid-body system moves on a rough plane. The inertial Cartesian coordinate frame Oi_1i_2 is fixed on the contact plane, where i_1 and i_2 represent the tangential and normal direction, respectively. The coordinate components (x_1, x_2) of the contact point in Oi_1i_2 can be expressed by generalized coordinates $(q_1, q_2, \ldots, q_n)$

$$x_i = x_i(q_1, q_2, \ldots, q_n), \quad \text{where} \quad (i = 1, 2) \tag{1}$$

In terms of Euler–Lagrange Equations, the dynamical equations can be written by

$$\ddot{\mathbf{q}} = \mathbf{M}^{-1}\mathbf{K}\mathbf{F} + \mathbf{M}^{-1}(-\mathbf{R} + \mathbf{W}) \tag{2}$$

Where, $\mathbf{M}_{n\times n}$ is symmetric positive mass matrix, $\mathbf{W}_{n\times 1}$, $\mathbf{R}_{n\times 1}$ and $\mathbf{F}_{2\times 1}$ are the column matrix of generalized active forces, the inertial forces and the contact forces, respectively. $\mathbf{K}_{n\times 2}$ is the Jacobian matrix of the transformation equations (1) from the coordinates of the contact point to the generalized coordinates with elements $k_{ij} = \partial x_j/\partial q_i$.

We should notice that the contact forces are undetermined variables in Equation (2), thus, some complementary equations have to be provided in advance.

Differentiating Equation (1) twice, we have the acceleration vectors in tangential and normal direction at contact point

$$\ddot{\mathbf{x}} = \mathbf{K}^{\mathrm{T}}\ddot{\mathbf{q}} + \mathbf{S} \tag{3}$$

Where, $\mathbf{S} = [S_1 \quad S_2]^{\mathrm{T}}$ is the affixation terms produced by the second derivatives of the transformation equations (1)

$$S_i = \sum_{j=1}^{n}\sum_{k=1}^{n}\frac{\partial^2 x_i}{\partial q_j \partial q_k}\dot{q}_j\dot{q}_k$$

Substitution of (2) into (3) leads to

$$\ddot{\mathbf{x}} = \mathbf{Q}\mathbf{F} + \mathbf{K}^{\mathrm{T}}\mathbf{M}^{-1}(-\mathbf{R} + \mathbf{W}) + \mathbf{S}, \quad \text{where}$$
$$\mathbf{Q} = \mathbf{K}^{\mathrm{T}}\mathbf{M}^{-1}\mathbf{K} \tag{4}$$

Property 1. $\mathbf{Q}$ *is a symmetric and definite positive matrix.*

Proof: Since $\mathbf{M}$ is a symmetric positive matrix, and $\mathbf{K}$ is full-rank if the number of generalized coordinates is not less than two (otherwise, the system will have no freedom), it is obvious that $\mathbf{Q}$ is a symmetric and definite positive matrix. □

Table 1 The possible solutions to the normal contact force

Mode of the solution	A	B	Number of solutions	Normal contact force
M_s^1	>0	>0	Unique solution	0
M_s^2	>0	<0	Unique solution	$F_2 = -\frac{B}{A}$
M_s^3	<0	>0	Two solutions	$F_2 = 0$ or $F_2 = -\frac{B}{A}$
M_s^4	≤ 0	<0	No solution	$\emptyset$

The property of the matrix $\mathbf{Q}$ will help us to analyze the process of the tangential impact when the inconsistency of paradoxical situation appears.

Assume that the contact point initially slides on the rough plane. Dry friction at the contact point is represented by Coulomb law of sliding friction with constant friction coefficient μ_0, then the tangential friction force and the normal force have the following relationship:

$$F_1 = \mu \cdot F_2 \tag{5}$$

where $\mu = \mu_0$ if $\dot{x}_1 < 0$ and $\mu = -\mu_0$ if $\dot{x}_1 > 0$.

Then, we can express the differential equations (4) in the tangential and normal direction as follows:

$$\ddot{x}_1 = C(\mathbf{q}, \mu) \cdot F_2 + D(\mathbf{q}, \dot{\mathbf{q}}) \tag{6}$$

$$\ddot{x}_2 = A(\mathbf{q}, \mu) \cdot F_2 + B(\mathbf{q}, \dot{\mathbf{q}}) \tag{7}$$

where

$$A(\mathbf{q}, \mu) = \mu Q_{21} + Q_{22},$$

$$B(\mathbf{q}, \dot{\mathbf{q}}) = \mathbf{K}_2^{\mathrm{T}} \mathbf{M}^{-1}(-\mathbf{R} + \mathbf{W}) + S_2$$

$$C(\mathbf{q}, \mu) = \mu Q_{11} + Q_{12},$$

$$D(\mathbf{q}, \dot{\mathbf{q}}) = \mathbf{K}_1^{\mathrm{T}} \mathbf{M}^{-1}(-\mathbf{R} + \mathbf{W}) + S_1$$

$\mathbf{K}_1$ and $\mathbf{K}_2$ represent the first and second column of matrix $\mathbf{K}$. Under the assumption of impenetrability of unilateral constraint fixed in space, the normal component of acceleration and contact force should satisfy with the following complementary condition:

$$\ddot{x}_2 \geq 0, \qquad F_2 \geq 0 \quad \text{and} \quad \ddot{x}_2 \cdot F_2 = 0 \tag{8}$$

Equation (7) combining with (8) is the standard form of complementary problem. Since both A and B may be positive or negative due to the friction, there are four cases corresponding to the calculation of contact forces. Following [14, 15], we list the possible solutions of the normal contact force in Table 1.

For the case of indeterminacy M_s^3 related to the two solutions of the normal contact force, the numerical results based on deformable methods [19, 21] and theoretical analysis in [15] have confirmed the solution that the normal contact force equals zero should be selected. For the case of inconsistency M_s^4 related to the non-existence of solutions, there will be a shock at the contact point [10–13, 18, 19, 23].

Therefore, the only case that can keep the contact on the rough plane is M_s^2. Then, we can define an admissible set in the state space of the system where the contact can be kept.

Definition 1. Assuming that $\mathbf{s}(\cdot) = (\mathbf{q}(\cdot), \dot{\mathbf{q}}(\cdot))$ represents the state of the system, $\mathbf{s}(\cdot)$ is admissible at time t where $t \in (\tau_0, \tau_0 + \epsilon)$ if and only if $\mathbf{s}(t) \in \Phi$, where $\Phi = \{\mathbf{s}(t) | A > 0, B < 0\}$. Φ is defined as an admissible set in the state space of the system.

Analyzing the components of the coefficients A and B in LCP equation may help us to understand the causes of the bouncing motion appearing in robotic systems. In terms of Equation (7), we can find the value of A is related to the velocity-dependent friction coefficient μ, and the matrix Q which is only affected by the configuration variables in the state space. Therefore, the configuration of the system is the only factor influencing the value of the coefficient A for a given friction coefficient. This can provide a clue to comprehend such phenomenon: if we try to make a robotic manipulator touch on a moving body, the tip will jump immediately in some special configurations, and we usually have to adjust the configuration of the system to avoid its appearance. So we can say there are some regions in the configuration space that is related to the Painlevé paradox, which cannot be reached if the unilateral constraint is applied on the mechanical system.

In the case of M_s^1 relating to $A > 0$ and $B > 0$, the bouncing motion will also appear. But the detachment at the contact point in this case is due to the coefficient

B which is affected by the state variables and the external forces applied in the system. Therefore, such bouncing motion can be controlled by designing a properly controller.

Therefore, we can attribute the bouncing motion appearing in the robotic system into two causes: one that is due to the special configuration related to $A < 0$; the other that is due to the external active forces and inertial action related to $B > 0$.

3 LCP equations for a robotic system

In this section, we will present the LCP equations for a robotic system with single unilateral constraint, and focus on the following problem: can the paradox only appear in a large value of friction coefficient?

A two-link manipulator comes into contact with a rough belt moving with constant speed v_t is shown in Fig. 1. The two links have the same length l and mass m. The vertical distance from the fixed point O to the rough surface is H. Let τ_1 and τ_2 be the torsion acting on the joints O and A, respectively. We take the joint angles θ_1 and θ_2 as the generalized coordinates of the system, and F_x, F_y represent the contact forces in the tangential and normal direction. The inertial coordinate frame Oxy is attached at the joint O. The relationship between the coordinate components of the contact point B in inertial frame and the generalized coordinates is

$$x = l(\sin\theta_1 + \sin\theta_2), \qquad y = -l(\cos\theta_1 + \cos\theta_2) \tag{9}$$

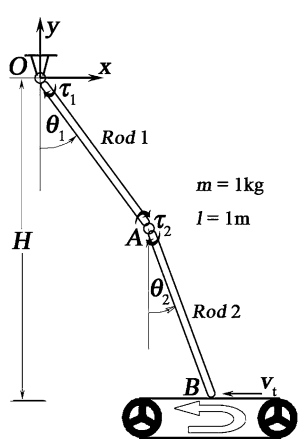

Fig. 1 Two-link manipulator touching on a moving belt

Then, the matrices of **K** and **S** in Equation (3) can be written by

$$\mathbf{K} = \begin{bmatrix} l\cos\theta_1 & l\sin\theta_1 \\ l\cos\theta_2 & l\sin\theta_2, \end{bmatrix},$$

$$\mathbf{S} = \begin{bmatrix} -l\left(\dot\theta_1^2\sin\theta_1 + \dot\theta_2^2\sin\theta_2\right) \\ l\left(\dot\theta_1^2\cos\theta_1 + \dot\theta_2^2\cos\theta_2\right) \end{bmatrix}$$

The kinetic energy of the robotic system

$$T = \frac{2}{3}ml^2\dot\theta_1^2 + \frac{1}{6}ml^2\dot\theta_2^2 + \frac{1}{2}ml^2\dot\theta_1\dot\theta_2\cos(\theta_1 - \theta_2)$$

The coefficient matrices in the dynamical equation (2) are

$$\mathbf{M} = \begin{bmatrix} 4ml^2/3 & ml^2\cos(\theta_1 - \theta_2)/2 \\ ml^2\cos(\theta_1 - \theta_2)/2 & ml^2/3 \end{bmatrix}$$

$$\mathbf{W} = \begin{bmatrix} \tau_1 - \tau_2 - 3mgl\sin\theta_1/2 \\ \tau_2 - mgl\sin\theta_2/2 \end{bmatrix},$$

$$\mathbf{R} = \begin{bmatrix} ml^2\dot\theta_2^2\sin(\theta_1 - \theta_2)/2 \\ ml^2\dot\theta_1^2\sin(\theta_1 - \theta_2)/2 \end{bmatrix}$$

The relative tangential velocity at contact point can be expressed as

$$\dot x_r = l(\dot\theta_1\cos\theta_1 + \dot\theta_2\cos\theta_2) - v_t \tag{10}$$

If there is relative movement between the tip of the robotic system and the belt, in terms of the Coulomb's frictional law, we can establish the complementary equation for determining the normal contact force.

$$\ddot y = AF_y + B \tag{11}$$

where,

$$A = l\sin\theta_1\frac{g_1(\theta_1,\theta_2,\mu)}{f(\theta_1,\theta_2)} + 4l\sin\theta_2\frac{g_2(\theta_1,\theta_2,\mu)}{f(\theta_1,\theta_2)}$$

$$B = l\sin\theta_1\frac{h_1(\theta_1,\theta_2,\dot\theta_1,\dot\theta_2)}{f(\theta_1,\theta_2)} + 4l\sin\theta_2\frac{h_2(\theta_1,\theta_2,\dot\theta_1,\dot\theta_2)}{f(\theta_1,\theta_2)} + l\dot\theta_1^2\cos\theta_1 + l\dot\theta_2^2\cos\theta_2$$

Functions f, g_1, g_2, h_1 and h_2 are shown in Appendix A. Obviously, the value of A is only related

to the configuration variables of the system and the velocity-dependent friction coefficient μ; while the value of B will be affected by the state variables and external active forces.

Meanwhile, the normal contact force and acceleration should satisfy the complementary condition if the contact between the tip of the manipulator and the moving belt is holding:

$$\ddot{y} \geq 0, \qquad F_y \geq 0, \quad \ddot{y} \cdot F_y = 0 \tag{12}$$

In terms of Equations (10) and (12), the critical value of the friction coefficient μ_m for just making $A = 0$ is

$$\mu_m = \left| \frac{4\left[3\cos\theta_1 - \theta_2 \sin\theta_1 \sin\theta_2 - \left(\sin\theta_1{}^2 + 4\sin\theta_2{}^2\right)\right]}{\sin(2\theta_1) - 5\sin(2\theta_2)} \right| \tag{13}$$

The reason of taking an absolute value for μ_m is as follows: if the critical friction coefficient is calculated with a negative value, it means in such configuration the paradoxical situation will appear only when the relative motion at the contact point reverses its direction assumed initially.

Since there is the following geometrical relationship between the joint angles, θ_1, θ_2, and the height H

$$l(\cos\theta_1 + \cos\theta_2) = H \tag{14}$$

For each constant height H, which is limited in $[0, 2l]$, the minimum of the critical friction coefficient $\mu_m^{\min}$ can be calculated by Equations (14) and (13). The change of $\mu_m^{\min}$ with the variation of height H is shown in Fig. 2.

From Fig. 2 we can find for such robotic system the paradoxical situation may appear even in a very small value of the friction coefficient. The minimum of the critical friction coefficient will decrease with the height increasing, particularly, the critical value can approach zero if the height of the system approaches $2l$.

The summary of this section is that even in a very small value of the coefficient of friction, the rigid dynamical equations in some configuration may also have no solutions or multiple solutions, which is influenced by the configuration of the system and the value of the friction coefficient as well as the direction of the relative motion at contact point. Since the paradoxical situation corresponds to the contact separating, some bouncing motion appearing in robotic system will be related to the Painlevé problem.

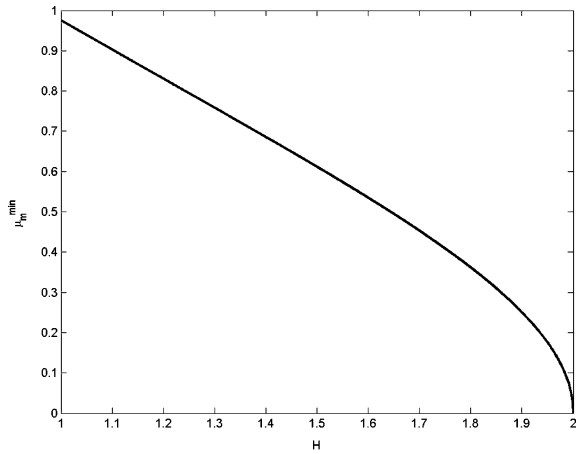

Fig. 2 The change of $\mu_m^{\min}$ with height

4 The admissible set and the properties of the dynamical equation at singular points

Based on the above description, we have the knowledge that the value of the friction of coefficient will influence the properties of the solutions of LCP equations. In this section, we will investigate the effect of the friction coefficient on the admissible set defined in the state space of the system. In the meantime, the following problem will be given attention: some bouncing motion may be appearing during slip, then we want to know whether such bouncing motion is related to the paradoxical situation. In other words, can the states of the system enter into M_s^3 or M_s^4 from M_s^2?

In terms of the geometrical relationship in Equation (14), for a fixed height H, we can express θ_2 as a function with respect to θ_1:

$$\theta_2 = \arccos(H/l - \cos\theta_1), \quad \dot{\theta}_2 = -\dot{\theta}_1 \sin\theta_1 / \sin\theta_2 \tag{15}$$

Then, the coefficient A can be expressed as a function with θ_1, while B is related to θ_1 and $\dot{\theta}_1$. Thus, the change of the coefficient A and B with the states of the robotic system can be reflected in the θ_1–$\dot{\theta}_1$ plane. In this, we can restrict $\theta_2 > 0$ as the configuration of the system will be symmetric to the Oy axis for $\theta_2 < 0$. The dynamical equation of the system can be expressed

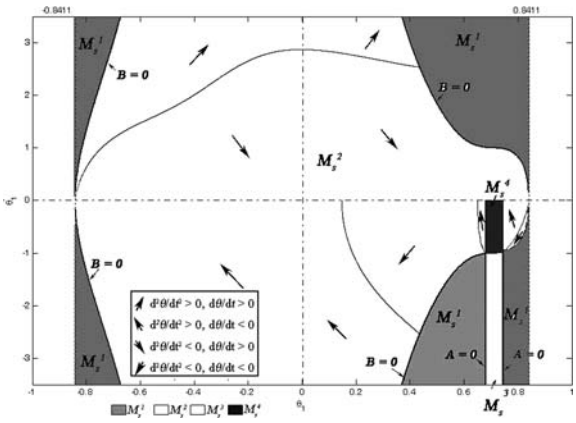

Fig. 3 The admissible set for $\mu = 0.5$

as follows when the tip is acted by Coulomb's friction force for slip:

$$\ddot{\theta}_1 = -\frac{\hat{g}_1}{\hat{f}}\frac{\hat{B}}{\hat{A}} + \frac{\hat{h}_1}{\hat{f}} \tag{16}$$

The notation $(\hat{\cdot})$ means the variables θ_2 and $\dot{\theta}_2$ involved in $(\cdot)$ will be replaced by θ_1 and $\dot{\theta}_1$ in terms of Equation (15).

Let the physical parameters of the two-link manipulator $H = 5/3\,\mathrm{m}$, $l = 1\,\mathrm{m}$, $m = 1\,\mathrm{kg}$, $g = 9.8\,\mathrm{m/s^2}$, $\tau_1 = \tau_2 = 0.0\,\mathrm{Nm}$, and assume that there is always a relative motion at the contact point, which will make the dynamical equation (16) come into existence. In terms of geometrical configuration of the system, the value of θ_1 will be limited in the scope of $[-0.8411, 0.8411]$. The minimum of critical friction coefficient is 0.4807 by Equation (13). The admissible sets for three typical values of coefficient of friction are presented as follows.

Case 1 ($\mu = 0.5$). The distributions for M_s^i in the θ_1–$\dot{\theta}_1$ plane are shown in Fig. 3. We can find the admissible set (M_s^2) keeping the end of the manipulator contact with the belt occupies the most area of the θ_1–$\dot{\theta}_1$ plane, and the paradoxical situation only appears in a very narrow strip, and is related to the direction of the relative motion ($\dot{\theta}_1 < 0$).

For answering the question presented in the start of this section, we should study the properties of the singular point at $\hat{A} = 0$ and $\hat{B} = 0$ in LCP equation, rewrite the dynamical equation Equation (16) by letting $x_1 = \theta_1(t)$ and $x_2 = \dot{\theta}_1(t)$.

$$\begin{cases} \dfrac{dx_1}{dt} = dx_2 \\ \dfrac{dx_2}{dt} = -\dfrac{\hat{g}_1}{\hat{f}}\dfrac{\hat{B}}{\hat{A}} + \dfrac{\hat{h}_1}{\hat{f}} \end{cases} \tag{17}$$

Introducing a singular transformation $dt = \hat{A}\,d\tau$, we can express Equation (17) as

$$\begin{cases} \frac{dx_1}{d\tau} = \hat{A}x_2 = w_1(x_1, x_2) \\ \frac{dx_2}{d\tau} = -\frac{\hat{g}_1}{\hat{f}}\hat{B} + \hat{A}\frac{\hat{h}_1}{\hat{f}} = w_2(x_1, x_2) \end{cases} \tag{18}$$

By using Taylor series expansion for Equation (18), we can get the Jacobian matrix J at the singular point of $\hat{A} = 0$ and $\hat{B} = 0$ for the linearization model of Equation (18):

$$\mathbf{J} = \begin{bmatrix} \frac{\partial w_1}{\partial x_1} & \frac{\partial w_1}{\partial x_2} \\ \frac{\partial w_2}{\partial x_1} & \frac{\partial w_2}{\partial x_2} \end{bmatrix}_{\hat{A}=0,\hat{B}=0} = \begin{bmatrix} \frac{\partial \hat{A}}{\partial x_1} & 0 \\ -\frac{\hat{g}_1}{\hat{f}}\frac{\partial \hat{B}}{\partial x_1} + \frac{\hat{h}_1}{\hat{f}}\frac{\partial \hat{A}}{\partial x_1} & -\frac{\hat{g}_1}{\hat{f}}\frac{\partial \hat{B}}{\partial x_2} \end{bmatrix}_{\hat{A}=0,\hat{B}=0}$$

For the case of $\mu = 0.5$, there are two singular points related to $\hat{A} = 0$ and $\hat{B} = 0$: $P_c^1 = (0.6819, -1.006)$, $P_c^2 = (0.744, -0.982)$. At point P_c^1, the eigenvalues of matrix J are $\lambda_1 = 1.273$ and $\lambda_2 = 22$; while at point P_c^2, $\lambda_1 = -1.379$ and $\lambda_2 = 22$. Therefore, P_c^1 is an unstable sink point and P_c^2 is a saddle point. This illustrates that the state of the system cannot enter into M_s^3 or M_s^4 if it is initially located in the region M_s^2. In other words, the bouncing motion appearing in slip for the planar robotic system is not due to the Painlevé problem. The similar conclusion has been found in study of the classical Painlevé example [15]. Figure 4 shows the numerical results by setting the initial states in the region M_s^2, which also verify such conclusion.

Case 2 ($\mu = 0.8$). The area for M_s^3 and M_s^4 in the θ_1–$\dot{\theta}_1$ plane will be extended accompanying with the increase of the value of the friction coefficient. We first determine the critical value of the friction coefficient for a special configuration that the two links are aligned in the same line. The angular for such

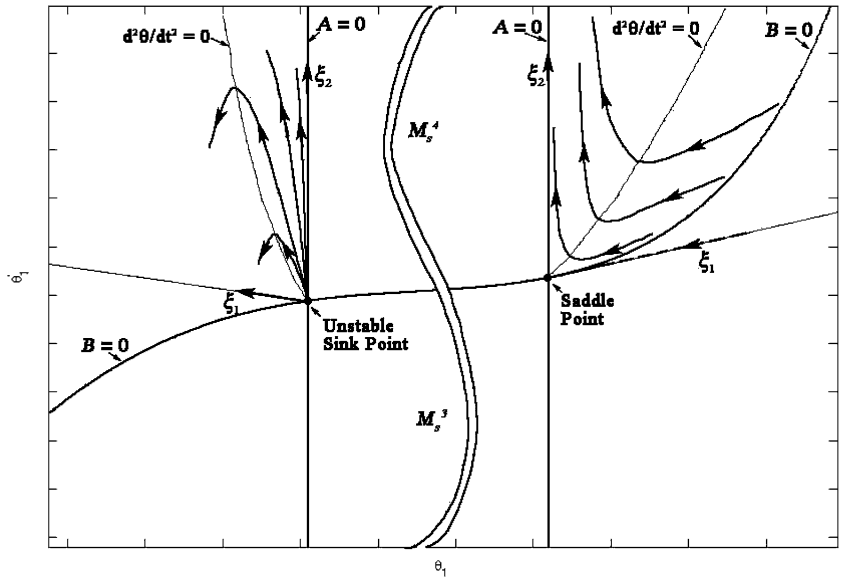

Fig. 4 The properties at singular point for $\mu = 0.5$

configuration will be

$$\theta^* = \theta_1 = \theta_2 = \arccos\frac{H}{2l}$$

In terms of Equation (13), the critical friction coefficient $\mu_0^\star$ for making $\hat{A} = 0$ in the configuration will equal

$$\mu_0^\star = \frac{\sqrt{4l^2 - H^2}}{H} \tag{19}$$

For the given structure parameters of the robotic system, $\mu_0^\star = 0.633$ and $\theta^* = 0.5857$. Figure 5 shows the distribution for the solution of LCP in the θ_1–$\dot{\theta}_1$ plane. Comparing Fig. 5 with Fig. 3, we can find that with the increase of the friction coefficient, the configuration related to the paradoxical situation will extend from a bigger value of θ_1 to a smaller one, and approach the special configuration that the two links are aligned. If $\mu > \mu_0^\star$, paradox will appear in the other side of the special configuration when the relative motion at the contact point reverse its direction ($\dot{\theta}_1 > 0$).

In Fig. 5, there are also two singular points: (0.5266, 1.6153) and (0.7944, −0.8617), both of them are saddle points according to the eigenvalues of the matrix J. Therefore, the states of the system cannot enter into the paradoxical area from M_s^2, even in a larger value of the friction coefficient.

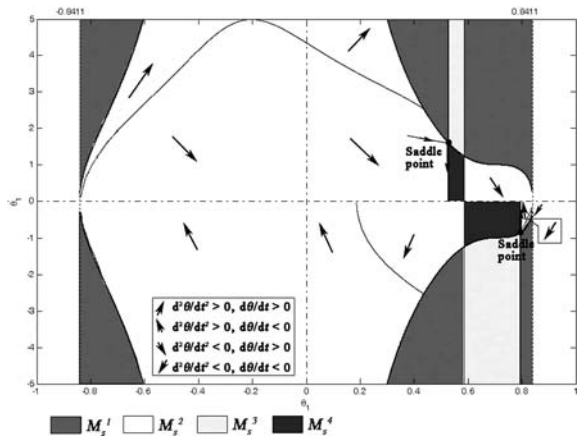

Fig. 5 The admissible set for $\mu = 0.8$

Case 3 ($\mu = 1.2$). With the increase of the value of friction coefficient, the region of $\hat{A} < 0$ will be further enlarged and even occupy the most part of the θ_1–$\dot{\theta}_1$ plane. From Fig. 6, we can find the region for M_s^3 and M_s^4 will be symmetric to the line of the special configuration when $\theta_1 > 0$, and will appear in the other side of the symmetrical line of the configuration ($\theta_1 < 0$) in the condition of $\dot{\theta}_1 > 0$. Therefore, the area for the occurrence of paradox is not continuous in the θ_1–$\dot{\theta}_1$ plane, and be dramatically influenced by the value of friction coefficient. The similar property that the robotic system cannot enter into the paradoxical area from M_s^2 also be found in such case.

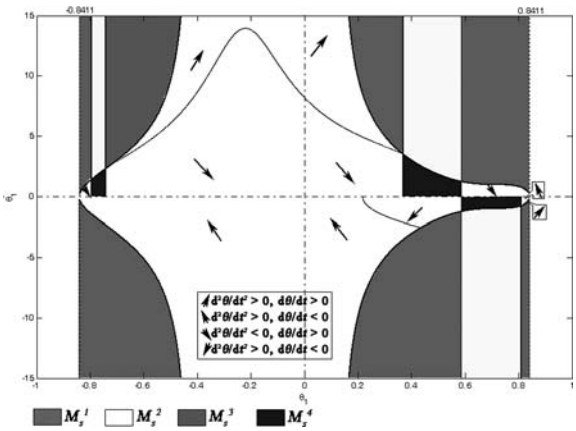

Fig. 6 The admissible set for $\mu = 1.2$

In summary, we use three typical values of friction coefficient to study its influences on the admissible set for the robotic system with a relative motion at contact point. The area for the occurrence of paradox on the θ_1–$\dot{\theta}_1$ plane will be enlarged and not continuous with the increase of the value of friction coefficient. Whether the paradoxical situations appear depends on the configuration of the system and the direction of slip at contact point for a given friction coefficient. Based on the properties of the singular points at $\hat{A} = \hat{B} = 0$ and numerical results, we can confirm that the robotic system cannot enter into the area of paradox from a slip mode, in other words, the bouncing motion generated by the paradoxical situation only occurs when the initial configuration of the system is located in the area of $\hat{A} < 0$; while the bouncing motion appearing in the process of slip is due to the external forces and inertial action.

5 The property of the tangential impact and the velocity jump rule

Once the Painlevé paradox occurs, the rigid-body model cannot provide an effective solution for dynamical simulation. Therefore, we should develop some theories to fill in the flaw existing in rigid-body dynamics. Based on the existing researches [13, 23], we have known that the indeterminacy in Painlevé paradox can be solved by selecting the contact force equals zero as a reasonable solution; while the inconsistent case will be related to a shock at contact point. In this section, we will study the properties of the tangential impact, and make attempt to develop some methods to rule out the paradoxical situation in using rigid-body model.

To be consistent with a shock, we probably need to use the method of impulsive dynamics to study the problem of tangential impact. But directly applying the collision law, such as the Newton's restitution coefficient, to solve such problem is helpless for determining the post-states as the relative normal speed equals zero before the tangential impact occurs. Fortunately, Keller [30] developed a general method in dealing with the problem of the collision between two rigid bodies with friction, which describes the impact process as a set of differential equations with respect to the normal impulse. This method provides a clue for analyzing the problem of tangential impact.

Taking advantage of the assumption of impulsive dynamics, the configuration of the system hardly changes during collisions, and the generalized impulse contributed by the finite forces is ignored. But we should discard the assumption of instantaneous impact in order to consider the impact as a continuous process with time. Integrating the dynamical equation (4) over a small interval of time, we can obtain a set of impulsive equations:

$$\begin{cases} d\dot{x}_1 = Q_{11} dP_1 + Q_{12} dP_2 \\ d\dot{x}_2 = Q_{21} dP_1 + Q_{22} dP_2 \end{cases} \tag{20}$$

where $d\dot{x}_1$ and $d\dot{x}_2$ are the changes of speed at contact point in tangential and normal direction during a small interval of time, dP_1 and dP_2 are the changes of tangential and normal impulses at the same time.

During tangential impact, if slip exists at contact point, the changes of the components in tangential impulse are related to the increment of normal impulse by the Coulomb's frictional law:

$$\frac{dP_1}{dP_2} = \mu \tag{21}$$

where $\mu = \mu_0$ if $\dot{x}_1 < 0$ and $\mu = -\mu_0$ if $\dot{x}_1 > 0$, and μ_0 is the friction coefficient. Then, the impulsive equations (20) can be expressed as the following form:

$$\begin{cases} d\dot{x}_1 = (\mu Q_{11} + Q_{12}) dP_2 \\ d\dot{x}_2 = (\mu Q_{21} + Q_{22}) dP_2 \end{cases} \tag{22}$$

Considering the fact that the normal impulse increases monotonously during impact, we can take it as a "time-like" variable [30–33]. Then, the normal

impulse dP_2 can be considered as independent differential variable. So Equation (22) represents the firs-order differential form of impulsive equations.

With respect to the property of Q and Equation (22), we have the following theorem.

Theorem 1. *If the tangential impact appears in a planar multibody system with single unilateral constraint, stick in tangential direction will occur at contact point after the impact finishes, and the process of tangential impact can be divided into three phases: sliding compressional period; sticking compressional period; sticking restitution period.*

Proof: In terms of the condition for the occurrence of tangential impact, we have

$$A = \mu Q_{21} + Q_{22} < 0$$

According to Property 1 for the matrix Q, which is a symmetric and definite positive matrix, there are some relationships for its elements:

$$Q_{22} > 0, \quad Q_{11} > 0, \quad \text{and}$$
$$Q_{11}Q_{22} > Q_{12}Q_{21} = Q_{21}^2$$

If we assume the tangential velocity $\dot{x}_1 < 0$, then $\mu = \mu_0 > 0$. Obviously, in such case only $Q_{21} < 0$ and $-\mu Q_{21} > Q_{22}$ can make $A < 0$. Then we have

$$-\mu Q_{21}Q_{11} > Q_{22}Q_{11} > Q_{21}^2$$

Thus, we can get $\mu Q_{11} > -Q_{21}$ and the coefficient in the second equation of (22), $C = \mu Q_{11} + Q_{12} > 0$. Therefore, if the tangential velocity $\dot{x}_1 < 0$ when the tangential impact starts, the coefficient $C > 0$. Similarly, if $\dot{x}_1 > 0$, we will obtain $C < 0$. Thus, whether $\dot{x}_1 < 0$ or $\dot{x}_1 > 0$, the tangential velocity will finally converge to zero during the tangential impact.

Once the tangential velocity equals zero, in terms of Equation (20) and setting $d\dot{x}_1 = 0$, we can get the ratio of the impulsive increment in tangential direction to the one in normal direction:

$$\frac{dP_1}{dP_2} = -\frac{Q_{12}}{Q_{11}} < \mu$$

The above expression shows that the contact impulse will be contained in the interior of the cone of friction, so stick in tangential direction will occur at the contact point once the tangential speed vanishes.

According to the second equation of (22), we can find a negative normal speed towards the rigidity contact plane before the tangential speed vanishes. It is not strange that the tangential movement will result in a compression in the normal direction at contact point although its initial value equals zero. Such results are consistent with the physical phenomena discovered by the methods of deformable elements [19, 23].

Therefore, if we adopt the Poisons's definition of collision as the terminal condition of impact, and divide the normal motion into compression phase and restitution phase, the process of tangential impact is composed of three periods: the first one is the *sliding compressional period* from the start of the tangential impact to the moment that slip vanishes; the second one is the *sticking compressional period* from the moment that slip just vanishes to the finish of compression phase in normal motion; the third one is the *sticking restitution period* from the moment that compression phase finishes to the end of the whole impact. □

Based on the property of tangential impact and the impulsive differential equation, we can develop a velocity jump rule for determining the post-states of the system after the tangential impact finishes.

5.1 Sliding compressional period

Let $\dot{x}_1^0$ be the initial slip speed of contact point. In terms of Theorem 1, the value of tangential speed will converge to zero during this period. Since Q can be considered as a constant matrix and by the first equation of (22), the normal impulse at the end of this period, P_2^1 can be expressed by

$$P_2^1 = -\frac{\dot{x}_1^0}{\mu Q_{11} + Q_{12}} \tag{23}$$

The normal speed at the end of this period can be obtained by the second equation of (22) and the condition that the initial speed in normal direction equals zero:

$$\dot{x}_2^1 = (\mu Q_{21} + Q_{22})P_2^1 \tag{24}$$

5.2 Sticking compressional period

In this period, stick will be held as the contact force is contained in the interior of the cone of friction. So we

should adopt Equation (20) rather than Equation (22), and set $d\dot{x}_1 = 0$. Then

$$\begin{cases} \frac{dP_1}{dP_2} = -\frac{Q_{12}}{Q_{11}} \\ d\dot{x}_2 = \left(-\frac{Q_{12}^2}{Q_{11}} + Q_{22}\right) dP_2 \end{cases} \tag{25}$$

Since the normal speed at the end of this period equals zero ($\dot{x}_2 = 0$), the increment of the normal impulse during this period can be obtained by integrating the above equation:

$$P_2^2 = \frac{Q_{11}\dot{x}_2^1}{Q_{12}^2 - Q_{11}Q_{22}} \tag{26}$$

5.3 Sticking restitutional period

During this period, the normal motion will restitute, and the contact will separate at the end of this period. In terms of Poisson's coefficient of restitution e_p, the increment of normal impulse of this period can be expressed as

$$P_2^3 = e_\mathrm{p}\left(P_2^1 + P_2^2\right) \tag{27}$$

Since stick in tangential direction is still kept at the end of this period, the separate speed at contact point after tangential impact finishes is

$$\dot{x}_1^f = 0, \quad \dot{x}_2^f = \left(-\frac{Q_{12}^2}{Q_{11}} + Q_{22}\right) P_2^3 \tag{28}$$

Obviously, there is a definite nonzero speed in the normal direction after impact if the coefficient of restitution e_p is not equal to zero, although its initial value equals zero.

So far, we have got the velocity jump rule for the tangential impact of planar multibody system with single unilateral constraint, which can be used for eliminating the paradox once the inconsistency case appears in using rigid-body model.

6 Simulation for the robotic system

In this section, we will comprehensively simulate the dynamical behavior of the two-link manipulator that comes into contact with a constantly moving belt by adopting rigid-body model. Due to the bouncing motion or the stick-slip motion at the contact point, the dynamical process of the robotic system will be complex and composed of different modes of motion, such as the free motion without contact constraint, detaching from the contact plane, impact with the contact plane and the stick-slip movement on the contact plane. The different modes of movement can be identified by the states at contact point, which will correspond to different dynamical equations for simulation. Once a tangential impact occurs at contact point, we can use the jump rule developed in the above section to determine the post-states, and make the simulation continue.

For imitating the action of a controller, we take the torsion at the joints have the following forms:

$$\tau_1 = -C_1\theta_1, \qquad \tau_2 = K_r(\theta_1 - \theta_2) - C_2(\dot{\theta}_1 - \dot{\theta}_2) \tag{29}$$

where K_r is the stiffness coefficient of the torsion spring, C_1 and C_2 are the damping coefficient at the joints. If the coefficients of K_r, C_1 and C_2 can be adjusted, Equation (29) is similar to a PD controller applied in the robotic system.

The structure parameters of the two-link robotic system are the same as described in Section 4: $H = 5/3\,\mathrm{m}$, $l = 1\,\mathrm{m}$, $m = 1\,\mathrm{kg}$, $g = 9.8\,\mathrm{m/s^2}$. The coefficient of friction for slip is set $\mu = 0.5$, and the one for the stick is set $\mu_s = 0.8$. The robotic system with zero speed comes in contact with the moving belt. The numerical results relating to the following cases illustrate the dynamical behaviors of the robotic system: the first case will explain that the bouncing motion can be induced by the Painlevé paradox; the second case will show that the bouncing motion can also be generated by the external forces and the inertial action; the third case will be used for exhibiting the stick-slip phenomenon.

Case 4. (The bouncing motion due to the Painlevé paradox). We set the initial configuration of the robotic system as $\theta_1 = 0.7, \theta_2 = 0.4468$, and the coefficients of the spring and damper as $K_r = 150\,\mathrm{Nm/rad}$, $C_1 = C_2 = 2\,\mathrm{Nm\,s/rad}$, the speed of the moving belt is $v_t = -0.4\,\mathrm{m/s}$. The initial values of the coefficients in LCP equation are $A = -0.0167$ and $B = -3.492$, which is located in the inconsistent region M_s^4. So

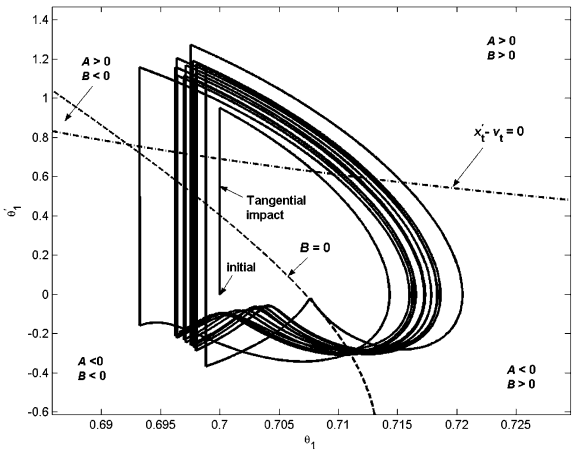

Fig. 7 Bouncing motion due to Painlevé paradox (phase trajectory in $e_p = 0.7$)

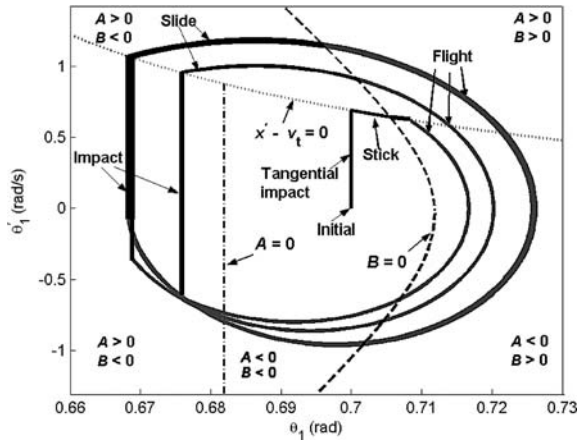

Fig. 10 Bouncing motion due to Painlevé paradox (phase trajectory in $e_p = 0$)

a tangential impact at contact point will occur when the end of the robotic system touches on the moving belt. The Poisson' restitution coefficient is set as $e_p = 0.7$.

Figure 7 shows the phase trajectory of the robotic system in $(\theta_1, \dot{\theta}_1)$ plane. Figures 8 and 9 show the speed of the end of the robotic system in tangential and normal direction. We can find the tip of the robotic system immediately detaches from the belt when it comes in contact, and the separating speed in tangential direction equals the value of the moving belt, while the separating speed in normal direction with a finite value. The initial detachment at the tip of the robotic system results in the subsequential bouncing motion with a characteristic of the quasi-periodic movement.

We adjust the controllable parameters $K_r = 100\,\text{Nm/rad}$ and $C_1 = C_2 = 0.1\,\text{Nm s/rad}$, and set the Poisson' restitution coefficient $e_p = 0$. From the phase trajectory shown in Fig. 10, we can find due to $e_p = 0$ the tip of the robotic system will stick on the belt after

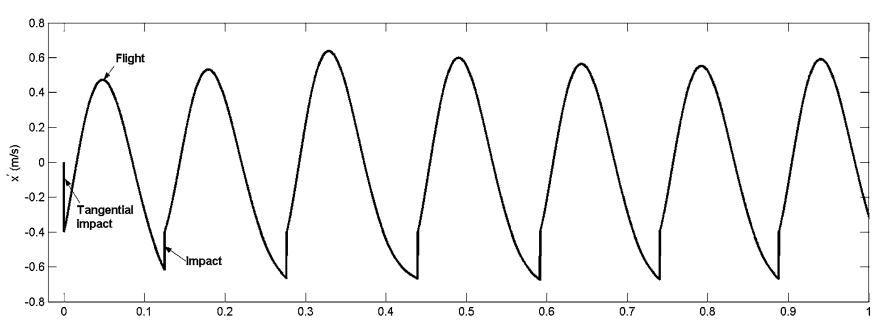

Fig. 8 Bouncing motion due to Painlevé paradox (tangential speed of the tip in $e_p = 0.7$)

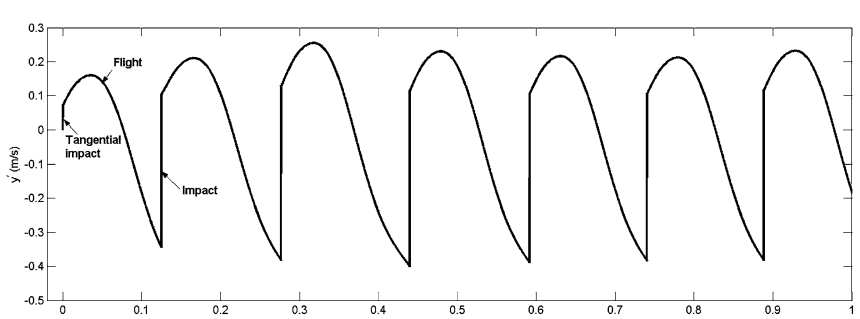

Fig. 9 Bouncing motion due to Painlevé paradox (normal speed of the tip in $e_p = 0.7$)

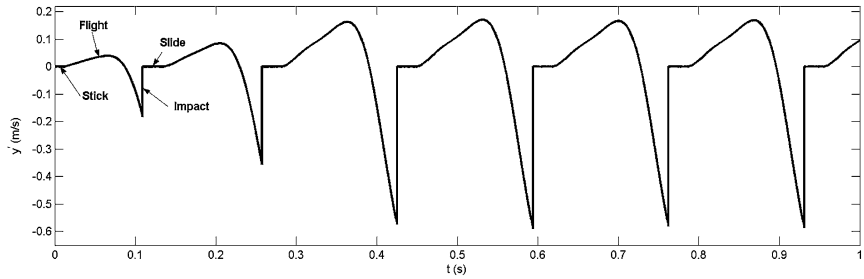

Fig. 11 Bouncing motion due to Painlevé paradox (tangential speed of the tip in $e_p = 0$)

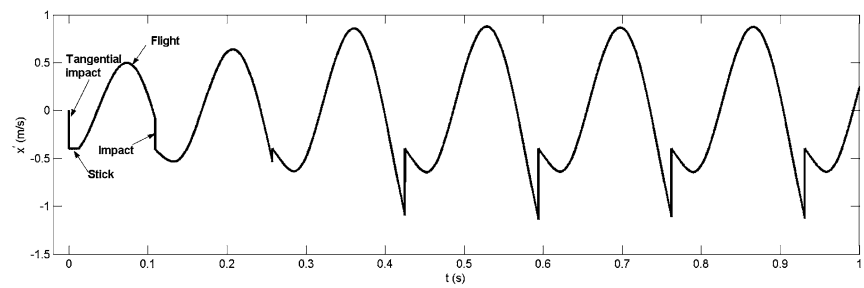

Fig. 12 Bouncing motion due to Painlevé paradox (normal speed of the tip in $e_p = 0$)

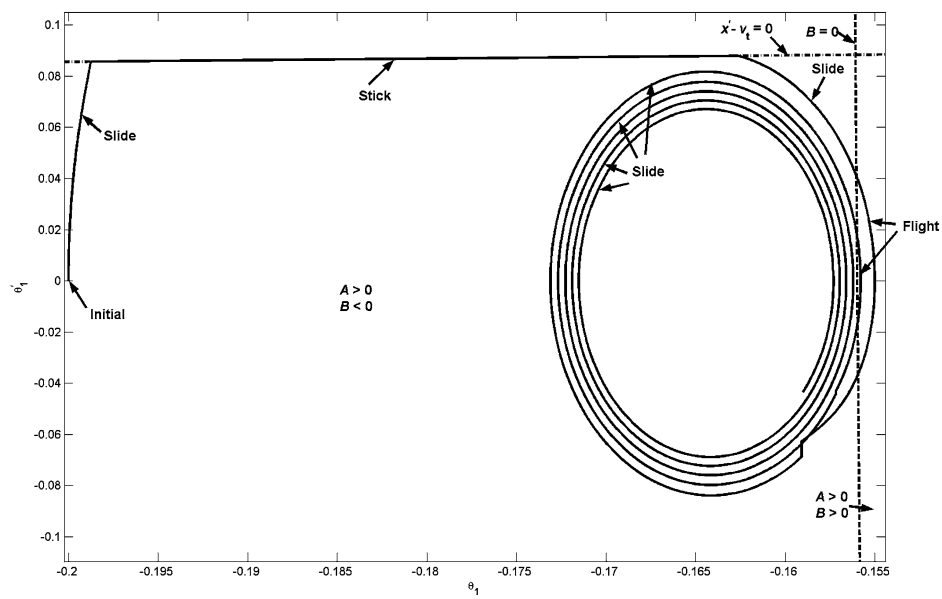

Fig. 13 Bouncing motion due to external action (phase trajectory)

the tangential impact finishes, which will lead to the conclusion that the kinetic energy of the blet is continuously transferred into the potential energy of the torsion spring. When the energy in joints is large enough to make the coefficient $B > 0$, a detachment at the tip will appear. Due to the action of the gravity and the spring at the joint, the tip will return to come in collision with the blet, and then slip on it as the collision is fully nonelastic. Once the phase trajectory meets the curve of $B = 0$, the tip will detach from the belt again. In this case, the tangential impact does not directly result in the detachment. But the stick at the contact point induced by it is just about the reason for the occurrence of bouncing motion appearing subsequently. So we can also attribute the bouncing motion in this case to the Painevé problem. The speed of the tip related to this example is shown in Figs. 11 and 12.

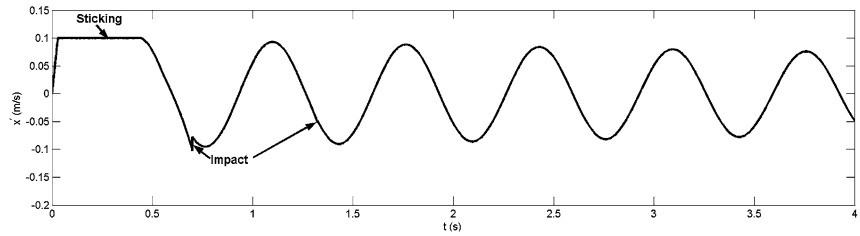

Fig. 14 Bouncing motion due to external action (tangential speed of the tip)

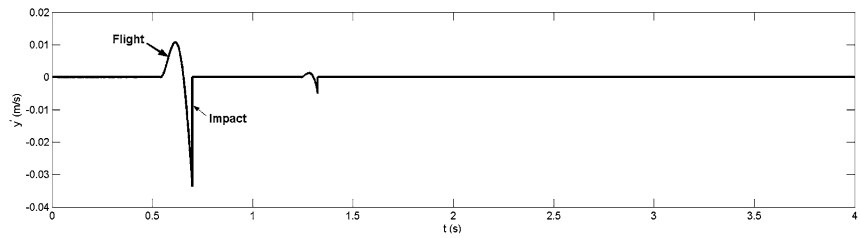

Fig. 15 Bouncing motion due to external action (normal speed of the tip)

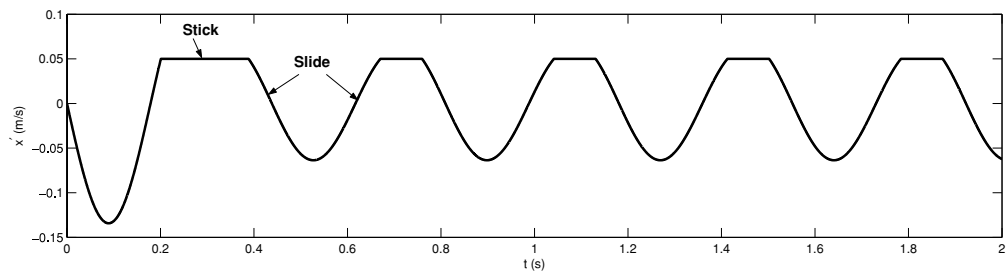

Fig. 16 The stick-slip motion

Case 5 (The bouncing motion that can be controlled). If the bouncing motion appears in the process of slip, in most cases it can be controlled. This can be illustrated by the following example: Let $\theta_1 = -0.2, \theta_2 = 0.4468$, $K_r = 100\,\text{Nm/rad}$, $C_1 = C_2 = 0.1\,\text{Nm s/rad}$, $e_\text{p} = 0$, and $v_t = 0.1\,\text{m/s}$. From Fig. 13 we can find the tip of the robotic system will firstly slide along the belt, then stick on it for a while, and will resume to slide. Once the trajectory meets the curve $B = 0$, the tip will detach from the belt and then return to come in collision with it. Only experiencing two impacts, the robotic system will be stabilized on the blet. Figures 14 and 15 show the speed of the tip in tangential and normal direction.

Case 6 (Stick-slip phenomenon). In some cases, even the detachment at the tip of the robotic system does not appear, the robotic system can still undergo stick-slip oscillation on the surface of the belt. Let $H = 4/3\,\text{m}$, $\theta_1 = 0.5$, $K_r = 100\,\text{Nm/rad}$, $C_1 = C_2 = 0.1\,\text{Nm s/rad}$ and $v_t = -0.05\,\text{m/s}$. The initial values of A and B are far away from the region of Painlevé paradox. Observing the tangential speed of the tip shown in Fig. 16, we can find a stick-slip phenomenon appearing: the tip will first slide backward, then reverse its direction of slip; when the speed of tip reaches the value of the belt speed, stick will occur and be kept for a time; accompanying with the increase of the joint energy transferred from the kinetic energy of the belt, the tip will get rid of the stick and resume to slip.

7 Conclusions

Bouncing motion can be often observed in mechanical system. Properly understanding such phenomena and providing effectively analytical tools in the framework of classical mechanics is very important for the control and dynamical analysis. The main conclusions of this paper are as follows.

First, we have established a general condition for identifying the occurrence of bouncing motion in a planar multibody system with single unilateral constraint,

and presented a definition of the admissible state set that the multibody system can keep contact. By analyzing the components of the coefficients in LCP equation, we can classify the bouncing motion appearing in the robotic system into two cases: one that is due to the special configuration of the system which is related to the Painlevé paradox; the other that is due to the external active forces and the inertial action.

We have found its application in an example of a two-link manipulator that comes in contact with a rough constantly moving belt, and investigated the structure of the admissible set and its changes with the shift of the value of friction coefficient. Numerical results shows that Painlevé paradox can appear even in a very small value of the coefficient of friction, and the region in the state space for its occurrence will be enlarged with the increase of friction coefficient. Based on the analysis of the singular points in LCP equation and the numerical simulation, we can confirm that the robotic system cannot enter into the area of paradox from a slip mode, in other words, the bouncing motion generated by the paradoxical situation only occurs when the initial configuration of the system is located in the area of Painlevé paradox.

Second, following the Keller's method for dealing with the collision between two rough bodies, we take the process of the tangential impact in a planar multibody system into the velocity impulse space with a first-order differential form of impulsive equations. The properties of the tangential impact has been discovered, which shows that the tangential impact can be divided into three phases: the sliding compression period, the sticking compression period, and the sticking restitution period. By using the Poisson's definition of restitution as the terminal condition of impact, we further develop an effective velocity jump rule for eliminating the paradoxical situations in using rigid-body model.

Finally, we present some numerical simulation to exhibit the bouncing motion and stick-slip movement appearing in the robotic system. Numerical results show that the bouncing motion due to the Painlevé paradox cannot be controlled only by applying a PD controller at joints, while the bouncing motion due to external forces and inertial action can be stabilized on the contact plane. Meanwhile, stick-slip phenomenon will appear in some parameters, although the contact at contact point is still kept. Experimental study relating to such system is in progress.

Acknowledgements The supports of the National Science Foundation of China (10502009 and 60334030) are gratefully acknowledged.

Appendix A

$$
\begin{aligned}
f(\theta_1,\theta_2) &= -\frac{4}{3}ml^2+\frac{3}{4}ml^2\cos^2(\theta_1-\theta_2)\\
g_1(\theta_1,\theta_2,\mu) &= \frac{3}{2}l\cos(\theta_1-\theta_2)(\mu\cos\theta_2+\sin\theta_2)\\
&\quad -l(\mu\cos\theta_1+\sin\theta_1)\\
g_2(\theta_1,\theta_2,\mu) &= \frac{3}{8}l\cos(\theta_1-\theta_2)(\mu\cos\theta_1+\sin\theta_1)\\
&\quad -l(\mu\cos\theta_2+\sin\theta_2)\\
h_1(\theta_1,\theta_2,\dot\theta_1,\dot\theta_2) &= \frac{3}{8}ml^2\dot\theta_1^2\sin(2(\theta_1-\theta_2))\\
&\quad +\frac{1}{2}ml^2\dot\theta_2^2\sin(\theta_1-\theta_2)\\
&\quad -\frac{3}{4}mgl\sin\theta_2\cos(\theta_1-\theta_2)\\
&\quad +\frac{3}{2}mgl\sin\theta_1-\tau_1\\
&\quad +\left[\frac{3}{2}\cos(\theta_1-\theta_2)+1\right]\tau_2\\
h_2(\theta_1,\theta_2,\dot\theta_1,\dot\theta_2) &= -\frac{3}{32}ml^2\dot\theta_2^2\sin(2(\theta_1-\theta_2))\\
&\quad -\frac{1}{2}ml^2\dot\theta_1^2\sin(\theta_1-\theta_2)\\
&\quad -\frac{9}{16}mgl\sin\theta_1\cos(\theta_1-\theta_2)\\
&\quad +\frac{1}{2}mgl\sin\theta_2+\frac{3}{8}\cos\theta_2\tau_1\\
&\quad -\left[\frac{3}{8}\cos(\theta_1-\theta_2)+1\right]\tau_2
\end{aligned}
$$

References

1. Painlevé, P.: Sur les lois du frottement de glissement. Comptes Rendu Séances ÍAcad. Sci. **121**, 112–115 (1895)
2. Klein, F.: Zu Painleves kritik der coulombschen reibungsgesetze. Z. Math. Phys. **58**, 186–191 (1909)
3. Delassus, E.: Considérations sur le frottement de glissement. Nouv. Ann. Math. (4èmé série) **20**, 485–496 (1920)

4. Delassus, E.: Sur les lois du frottement de glissement. Bull. Soc. Math. France **51**, 22–33 (1923)
5. Lötstedt, P.: Coulomb friction in two-dimensional rigid-body systems. Z. Angew. Math. Mech. **61**, 605–615 (1981)
6. Lötstedt, P.: Mechanical systems of rigid bodies subject to unilateral constraints. ASME J. Appl. Math. **42**, 281–296 (1982)
7. Erdmann, M.: On a representation of friction in conguration space. Int. J. Robotics Res. **13**(3), 240–271 (1994)
8. Moreau, J.J.: Unilateral Contact and Dry Friction in Finite Freedom Dynamics. Nonsmooth Mechanics and Applications, pp. 1–82. Springer, Berlin Heidelberg New York (1988)
9. Wang, Y., Mason, M.T.: Two-dimensional rigid-body collisions with friction. J. Appl. Mech. **59**, 635–642 (1992)
10. Baraff, D.: Coping with friction for non-penetrating rigid body simulation. Comput. Graph. **25**(4), 31–40 (1991)
11. Glocker, C., Pheiffer, F.: Multibody Dynamics with Unilateral Contacts. Wiley, New York (1996)
12. Payr, M., Glocker, C.: Oblique frictional impact of a bar: analysis and comparison of different impact laws. Nonlinear Dyn. **41**, 361–383 (2005)
13. Brogliato, B.: Nonsmooth Mechanics, 2nd edn. Springer, Berlin Heidelberg New York (1999)
14. Leine, R.I., Brogliato, B., Nijmeijer, H.: Periodic motion and bifurcations induced by the Painlevé paradox. Eur. J. Mech. A Solids **21**, 869–896 (2002)
15. Génot, F., Brogliato, B.: New results on Painlevé paradoxes. Eur. J. Mech. A Solids **18**, 653–677 (1999)
16. Ivanov, A.P.: The problem of constrainted impact. J. Appl. Math. Mech. **61**(3), 341–253 (1997)
17. Ivanov, A.P.: Singularities in the dynamics of systems with non-ideal constraints. J. Appl. Math. Mech. **67**(2), 185–192 (2003)
18. Brach, R.M.: Impact coefficients and tangential impacts. ASME J. Appl. Mech. **64**, 1014–1016 (1997)
19. Zhen, Z., Bin, C., Liu, C., Hai, J.: Impact model resolution on Painlevé's paradox. ACTA Mech. Sin. **20**(6), 659–660 (2004)
20. Zhen, Z., Liu, C., Bin, C.: The numerical method for three-dimensional impact with friction of multi-rigid-body system. Sci. China Ser. G Phys. Astr. **49**(1), 102–118 (2006)
21. Peng, S., Kraus, P., Kumar, V., Dupont, P.: Analysis of rigid-body dynamic models for simulation of systems with frictional contacts. J. Appl. Mech. **68**, 118–128 (2001)
22. Grigoryan, S.S.: The solution to the Painlevé paradox for dry friction. Doklady Phys. **46**(7), 499–503 (2001)
23. Stewart, D.E.: Rigid-body dynamics with friction and impact. SIAM Rev. **42**(1), 3–39 (2000)
24. Stewart, D.E.: Convergence of a time-stepping scheme for rigid-body dynamics and resolution of Painlevé's problem. Arch. Rational Mech. Anal. **145**, 215–260 (1998)
25. Wilms, E.V., Cohen, H.: The occurence of Painlevé's paradox in the motion of a rotating shaft. J. Appl. Mech. **64** (1997)
26. Ibrahim, R.A.: Friction-induced vibration, chatter, squeal and chaos. Part II: Dynamics and modeling. ASME Appl. Mech. Rev. **47**(7), 227–253 (1994)
27. Brogliato, B.: Some perspectives on the analysis and control of complementarity systems. IEEE Trans. Autom. Control **48**(6), 918–935 (2003)
28. Schiehlen, W., Seiferied, R.: Three approaches for elastodynamic contact in multibody systems. Multibody Syst. Dyn. **12**, 1–16 (2004)
29. Hu, B., Eberhard, P., Schiehlen, W.: Comparison of analytical and experimental results for longitudinal impacts on elastic rods. J. Vib. Control **9**, 157–174 (2003)
30. Keller, J.B.: Impact with friction. Trans. ASME J. Appl. Mech. **53**, 1–4 (1986)
31. Stronge, W.J.: Impact Mechanics. Cambridge University Press, Cambridge, UK (2000)
32. Bhatt, V., Koechling, J.: Partitioning the parameter space according to different behaviors during three-dimensional. ASME J. Appl. Mech. **62**, 740–746 (1995)
33. Batlle, J.A.: Rough balanced collisions. ASME J. Appl. Mech. **63**, 168–172 (1996)